Are the 7 March 2006 *Mw* 5.6 event and the 3 February 2006 *Mw* 4.58 event triggered by the five years continued occurrence of aftershocks of the 2001 *Mw* 7.7 Bhuj event?

Prantik Mandal*, R. K. Chadha, I. P. Raju, N. Kumar, C. Satyamurty and R. Narsaiah

National Geophysical Research Institute, Hyderabad 500 007, India

We present the locations, *b*-values and aftershock decay parameters for the aftershock sequences of the 2001 *Mw* 7.7 Bhuj and the 2006 *Mw* 5.6 GEDI events. A study of temporal distributions (2001–06) of earthquakes along the North Wagad Fault (NWF), Island Belt Fault (IBF) and GEDI Fault (GF) enabled us to infer that the 3 February 2006 event along IBF at 28.7 km depth and the 7 March 2006 event along GF at 2.2 km depth were triggered by the five years continued aftershock activity subsequent to the 2001 event. Analysis of focal mechanisms suggests dominance of reverse movements on the south-dipping NWF and IBF, but strike-slip motion is observed along GF. The 7 March event gives a large stress drop of 26.7 MPa, whereas those on 17 and 19 February 2006 suggest smaller stress drop values of the order of 1.5 MPa. However, the 3 February event is associated with an anomalously large stress drop of 70.6 MPa. The *b*-value for the $M \geq 3$ Bhuj aftershock sequence (2001–05) is 0.77, but for the 2006 sequence it is 0.81. It is inferred based on these low *b*-values that both the aftershock sequences could be categorized as the MOGI's type-II sequences, indicating a region of intermediate-level stresses and heterogeneous rocks. The *p*-value or aftershock decay exponent is estimated to be 0.99 and 0.88 for the 2001–05 and the 2006 sequence respectively. This is less than the global median of 1.1, suggesting slower decay for these two studied aftershock sequences.

Keywords: Aftershocks, GEDI Fault, Island Belt Fault, *b*-value, *p*-value.

EARTHQUAKES have struck stable continental regions (SCRs) in plate interiors at several locations worldwide[1]. However, only at a few locations did the earthquakes cause surface ruptures: the Tennant Creek, Australia; Ungava, Canada, and 1819 Kachchh and 1993 Latur, India[1–3]. However, in most cases no surface ruptures are evident, including the latest 2001 Bhuj earthquake of *Mw* 7.7. Among the SCR regions worldwide, only the New Madrid and Kachchh regions[4] have experienced earthquakes of magnitude approaching 8. SCR earthquakes are quite rare, accounting for only 0.5% of the total annual seismic energy released globally[1]. However, these earthquakes can be devastating. The Bhuj earthquake of 26 January 2001 claimed about 14,000 lives, the 1993 Latur earthquake in Maharashtra killed 10,000 people and the 1997 Jabalpur earthquake claimed a hundred lives. These earthquakes generally have long return periods, which make their occurrences rare[5]. Thus, the occurrence of *M* 5.6 earthquake along the pre-existing GEDI Fault (GF) perhaps resulted from the continued aftershock activity along the North Wagad Fault (NWF) for more than five years. This provides a rare opportunity to study the physics of the two significantly different, but closely spaced aftershock sequences of intraplate earthquakes. Here we study the spatio-temporal distribution, *b*-value and *p*-value of the five years aftershock activity along the NWF, GF and Island Belt Fault (IBF) aimed at obtaining a better understanding of this unique aftershock sequence.

The frequency–magnitude distribution mainly defines the relative amount of smaller to larger earthquakes through its 'slope-parameter' *b*. This has been extensively studied in laboratory experiments, as well as for synthetic and real seismicity. There are three main natural factors, as inferred from laboratory studies, that can cause significant changes of the frequency–magnitude distribution from an average value of 1.0: (i) increased material heterogeneity increases the *b*-value[6]; (ii) increase in shear stress or effective stress decreases the *b*-value[7], and (iii) increase in the thermal gradient may cause an increase in the *b*-value[8]. High *b*-values are generally observed for highly cracked volumes like magma chamber, reservoir-induced or intraplate sites[9]. However, small *b*-value is observed for asperities or probable zones for future large earthquakes like plate boundaries. Another important parameter to characterize an aftershock sequence is the *p*-value, which is a measure of the decay rate of aftershocks, as described by the Omori law[10]. Worldwide review[11] of the *p*-value estimates

*For correspondence. (e-mail: prantikmandal@yahoo.com)

suggests a range from 0.6 to 2.5, with a median around 1.1. Regional variation of the p-value has been related to the variation in heat flow[6]. Variability of estimated p-values may be related to the structural heterogeneities, stress and temperature in the crust[11]. Hence, the estimation of b- and p-values for the complete Bhuj sequence could provide a much better understanding of the physical processes responsible for the continued aftershock activity for more than five years.

In this article, we present the salient results from the estimated hypocentral parameters of the aftershocks of the 2001 Bhuj earthquake of Mw 7.7 as well as aftershocks of the 7 March 2006 event of Mw 5.6. For the 2001 event, we have used 1238 aftershocks recorded by a combined network of the National Geophysical Research Institute (NGRI), Hyderabad, India and Centre for Earthquake Research and Information (CERI), Memphis, USA during 12–28 February 2001. Whereas for the 2006 aftershock sequence (7–11 March 2006), we have used data from a network of ten strong-motion accelerographs and five broadband stations. Finally, relocation of aftershocks, b- and p-values are correlated with the local geology and tectonics with a view to understand the causative mechanism of these aftershock sequences.

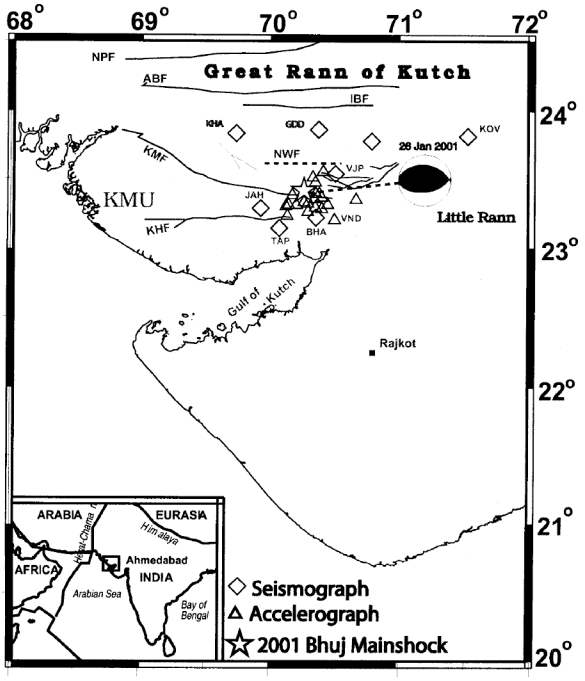

Figure 1. Map showing twenty accelerographs (open triangles) and six seismograph stations (open diamonds) along with the main shock epicentre (star). The focal mechanism solution of USGS showing reverse faulting on a south-dipping fault is also shown. The solid square marks Rajkot, Saurashtra, India. KMU, Kachchh Mainland Uplift. Major faults (lines): ABF, Allah Bund Fault; IBF, Island Belt Fault; KMF, Kachchh Mainland Fault; KTF, Katrol Hill Fault; NPK, Nagar Parkar Fault; NWF, North Wagad Fault; SWF, South Wagad Fault; GF, GEDI Fault. (Inset) Study area with reference to Indian plate boundaries (dark lines; modified after Biswas and Deshpande[13]).

The Kachchh rift is the largest Indian intracontinental rift zone and is situated at the western border of India far from any plate boundary (Figure 1). Geologically, Quaternary/Tertiary sediments, Deccan volcanic rocks and Jurassic sandstones resting on Archean basement mainly characterize the Kachchh region[12]. The Mesozoic rift-related extensional structures of the Kachchh basin got reactivated as strike-slip or reverse faults as a result of regional compressive stresses due to collision of Indian and Eurasian plates since Neogene times[13,14]. The focal mechanisms of some earthquakes indicate reverse faulting[14].

Major structural features of the Kachchh region include several E–W trending faults as shown in Figure 1. The rift zone is bounded by a north-dipping Nagar Parkar Fault in the north and a south-dipping Kathiawar Fault in the south. Other major faults in the region are the E–W trending Allah Bund Fault, IBF, Kachchh Mainland Fault and Katrol Hill fault. In addition, several NE and NW trending small faults/lineaments are observed[15]. Seismic, gravity and magneto-telluric surveys indicate undulated basement with 2–5 km deep sediments. In southern Kachchh region, crustal thickening or underplating has been noticed[12,16] in the models constructed from the refraction seismics, where the Moho depth varies from 35 to 43 km. Recently, analysis and inversion of teleseismic RF suggest a Moho depth variation from 40 to 49 km in the epicentral zone of the 2001 Bhuj earthquake[17], which is quite unusual for a rifted region. However, detailed tomographic study of the region also delineated mafic intrusive bodies extending from 5 to 35 km depth, supporting the thickening of crust in the region[18]. These tomographic studies also revealed that the 2001 Bhuj main shock nucleates in a low-velocity zone, suggesting the existence of overpressurized fluids[18–20]. In general, the 2001 Bhuj aftershock zone is tectonically complex, as it contains focal mechanisms of multiple orientations and different nature[19].

Until March 2006, 11 earthquakes of magnitude exceeding 5, over 170 earthquakes of magnitude exceeding 4 and several thousand earthquakes of magnitude ≤4 have occurred in the aftershock zone of 2001 Mw 7.7 Bhuj earthquake. This aftershock activity has been monitored by NGRI since 4 February 2001, with a local digital network consisting of eight 24-bit recorders with an external hard disk (2 GB) and GPS timing system. Among these six were equipped with short-period seismometers (frequency range 1–40 Hz) and two were equipped with broadband seismometers (frequency range 0.01–40 Hz). Recording was done in a continuous mode at 100 sps. Some station locations were shifted during the study period, making a total of 12 station sites. Further, we used data from the seismic network of CERI (from 13 to 27 February 2001) and Hirosaki University, Japan (from 28 February to 7 March 2001)[21]. The station locations of this combined network are shown in Figure 1. The distance between station and epicentres varies from 14 to 90 km. This network provides an azimuthal gap of less than 180°. Most of these stations were located

on hard sediments or rocks (Jurrassic sediments or basalt). However, a few of these stations were on a thin layer of soil overlying rock. The network is covered well in all directions, except the northern and central areas due to non-availability of roads in Banni region.

With a view to obtain a better understanding of the continued aftershock activity, seismic hazard, attenuation and source processes, NGRI deployed a new network consisting of ten strong-motion accelerographs and five broadband seismographs in August 2002. Again in February 2006, NGRI deployed another ten strong-motion accelerographs in the aftershock zone. Soon after the occurrence of 7 March 2006 event of *Mw* 5.6, NGRI deployed another three short-period digital seismograph stations for better monitoring of the aftershocks of the 7 March 2006 event (Figure 1). Since NGRI stations were closely spaced in the epicentral zone, at least one station was always within a distance of the hypocentral depth, which enabled good control on the focal depth estimation. Seventy per cent weight was assigned to impulsive clear *P*-picks, while 10% to weak emergent *P*-phases. The *P* to *S* converted phase was observed as weak *S*-arrivals, followed by a strong *S*. Avoiding the weak beginning of the *S*-wave train and picking up *S* at the strong arrival, *P* to *S* converted phase is excluded. A maximum of 50% weight was assigned to clear *S*-picks and 5% to weak *S*-phases. Strong events like 3, 17 and 19 February as well as the 7 March 2006 triggered 8–16 strong-motion accelerographs. As an example, we show the strong motion records for the 7 March 2006 *Mw* 5.6 event recorded at ten sites (Figure 2), which suggests a heterogeneous disposition of peak ground acceleration values in the aftershock zone, indicating wide variation in site effects.

Event locations were obtained using the HYPO71PC program and 1D velocity model obtained from the inversion of the receiver functions (RFs) of teleseismic *P*-waves at five broadband stations in the Kachchh basin. Details on inversion of RFs can be found in Mandal[17]. This velocity model is similar to that of Bodin and Horton[21], except for a shallow Moho depth (i.e. 39 km). The above-mentioned velocity models suggest a high-velocity mafic crust, which is in a good agreement with the observation of mafic intrusive bodies at 5–35 km depth as revealed by the tomographic study of the area[18]. The V_p/V_s ratio is fixed at 1.73. The initial velocity model consisting of nine layers is shown in Table 1.

During February 2001–July 2002, a total of 2000 aftershocks were located using *P*- and *S*-wave arrival time phase data from 5 to 18 three-component digital stations (Figure 3 *a*). The average rms of *P*-wave residual was 0.05 s. Mean horizontal and vertical, single, 90% confidence estimates are 1.5 and 2.5 km respectively, for the aftershocks. Figure 3 *a* shows that the aftershocks are distributed over a fairly broad area (90% of aftershock locations is confined to a 60×40 sq. km area), but that most epicentres fall within roughly trapezoidal shape with the parallel sides oriented east-west[21]. In cross-section (Figure 3 *b*) a south-dipping concentration of aftershocks is seen to extend from between 5 and 10 km deep to about 35 km deep. This south-dipping trend, i.e. NWF, appears to touch the surface about 25 km north of KMF, which is in agreement with the strike of another fault, mapped by Biswas[15], about 30 km east of the NWF, as shown in Figure 3 *a*. The east-west strike is about 8° from the WSW–ENE striking, south-dipping, nodal plane of the mainshock (Figure 1). It will be important to note that one *Mw* 2.2

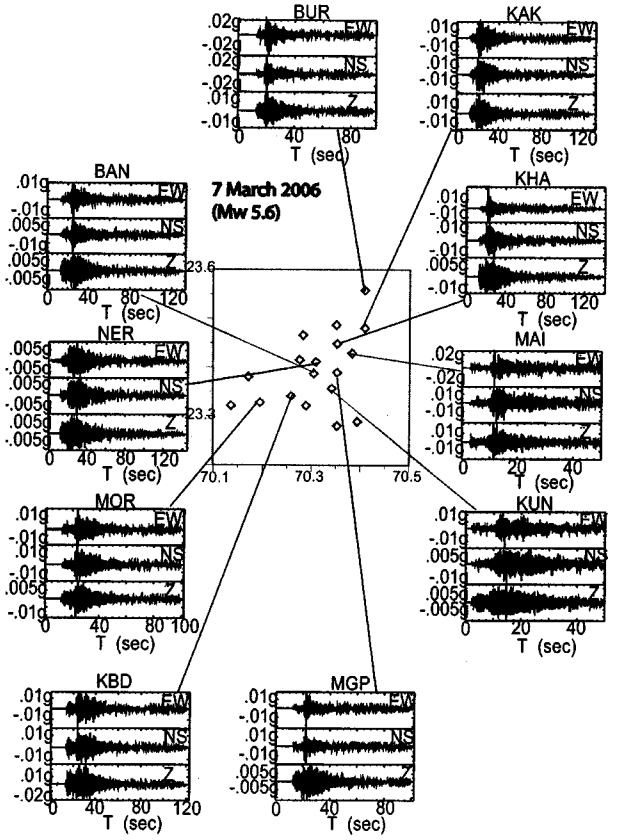

Figure 2. Plot showing the three-component accelerograms for 7 March 2006 event recorded at 10 SMA stations, namely BUR (Burudia), KAK (Kakarvada), KHA (Kharoi), KUN (Kunjisar), NER (Ner), BAN (Bandri), MAI (Mai), MGP (Meghpar), KBD (Kumbardi) and MOR (Morgar). This event was also recorded at another four SMA stations, namely Sivalakha, Bhachau, Sikara and Newdudhai, which are not plotted.

Table 1. One-dimensional velocity model obtained from inversion of RF

Depth to the top of layer (km)	*P*-wave velocity (km/s)
0.0	3.0
1.5	6.25
10.0	6.45
15.0	6.48
20.0	6.72
25.0	7.15
30.0	7.49
35.0	7.88
42.0	8.20

aftershock occurred along the GF in 2002 (Figure 3 *a*). There were also about 15 smaller aftershocks along the KMF during this period (Figure 3 *b*).

During August 2002–December 2003, a total of about 652 aftershocks, including ten *Mw* 4–4.6, 95 *Mw* 3–3.9, 403 *Mw* 2–2.9 and 144 *Mw* 1.1–1.9 events have been located using *P*- and *S*-wave phase data from 3 to 5 digital seismograph stations. For locating strong aftershocks, the *P*- and *S*-wave phase data from ten accelerographs were used (Figure 4 *a*). The rms errors in *P*-residual times are found to be less than 0.35 s, giving an error in epicentral location less than 1.5 km and error in focal depth estimation less than 2.5 km. The epicentres of the 652 aftershocks during 2002–03 define an almost east-west trending aftershock zone covering an area 100 × 100 sq. km (Figure 4 *a*), but 90% of aftershock locations is confined to a 60 × 50 sq. km area. Focal depths of these aftershocks vary from 2.5 to 56.8 km with 90% of the events occurring between 10 and 35 km depths (Figure 4 *b*). Thus, the aftershock zone during 2002–03 has increased spatially as well as depth-wise in comparison to the earlier aftershock zone during 2001. It will be important to note that some larger aftershocks began to occur along the GF in 2003. The 5 August 2003 event (*Mw* 4.5) and another six events of $M \leq 3.5$ that have occurred along the GF at 0–10 km depth may be considered as a manifestation of this activity (Figure 4 *b*). It is also noticed that 13 events have occurred along IBF at 20–50 km depth.

In 2004, a total of about 281 aftershocks, including five *Mw* 4–4.3, 70 *Mw* 3–3.9, 180 *Mw* 2–2.9 and 26 *Mw* 1.1–1.9 events have been located (Figure 5 *a*). During this period, the aftershock zone still defined an E–W trending zone extending from 3 to 40 km depth (Figure 5 *b*). However, activity along the GF became more with the occurrence of two *M*4 events, six *M*3 events, five *M*2 events and one *M*1 event (Figure 5 *b*). Activity along the IBF had also increased in 2004. There were two *M*4, three *M*3 and five *M*2 events along the IBF (Figure 5 *b*). In 2005, we located a total of about 585 aftershocks, including 16 *Mw* 4–4.5, 155 *Mw* 3–3.9, 394 *Mw* 2–2.9 and 20 *Mw* 1.1–1.9 events (Figure 6 *a*). During this period, again the aftershock zone defined an E–W trending zone extending from 3 to 40 km depth. However, activity along the GF was subdued with occurrences of one *M*3, three *M*2 and four *M*1 events (Figure 6 *b*). Activity along the IBF was also less in 2005. There were two *M*3 and six *M*2 events along the IBF.

In 2006, a total of about 42 aftershocks, including three *Mw* 4–4.6, 24 *Mw* 3–3.9 and 15 *Mw* 2–2.9 events were located (Figure 7 *a*). During this period, all events occurred in the aftershock zone of 2001 Bhuj earthquake, except the one on 3 February 2006 (*Mw* 4.58) along the IBF at 28.7 km depth (Figure 7 *b*). There were no events along the GF. However, the 7 March 2006 event of

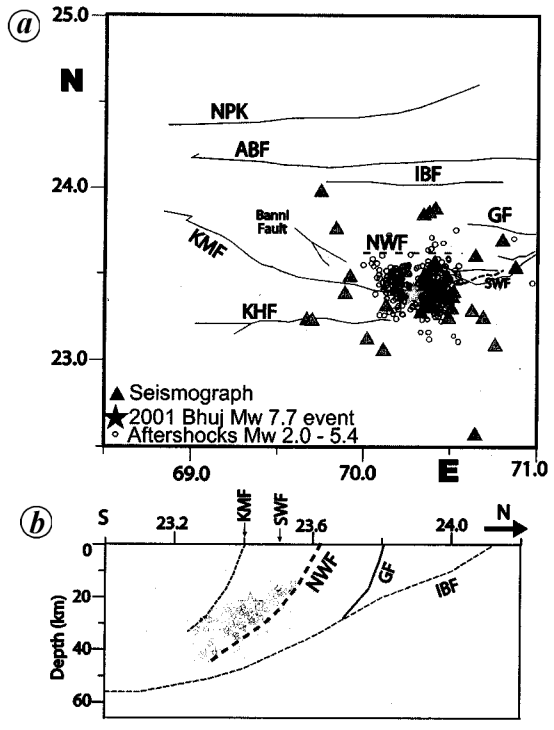

Figure 3. *a*, Epicentres of 2000 aftershocks using HYPO71PC, which have occurred during February 2001 to July 2002. Solid grey star shows the epicentre for the 2001 Bhuj mainshock. The inferred causative fault is shown by dotted line and marked as NWF. *b*, Hypocentral depth plot of earthquakes in N–S direction. (Geologically valid inferred fault traces are shown by dotted lines and marked as NWF and IBF. Surface trace of SWF is shown by arrow. The inferred geologically valid GF trace is shown by solid line (after Biswas[15]).)

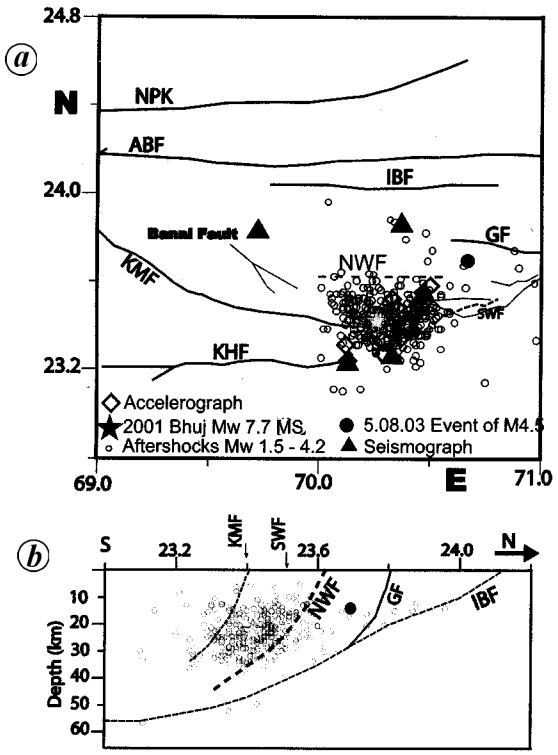

Figure 4. *a*, Epicentres of 652 aftershocks during August 2002–December 2003. Solid star shows epicentre for the 2001 Bhuj mainshock. *b*, Hypocentral depth plot of earthquakes in N–S direction.

Mw 5.6 and its 72 aftershocks (during 7–11 March 2006) occurred along the GF, which is about 20 km northeast of the causative NWF for the 2001 *Mw* 7.7 Bhuj earthquake.

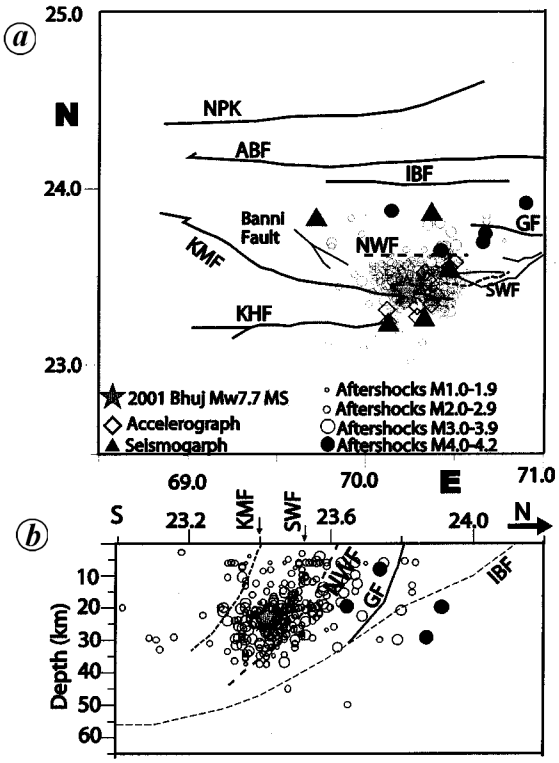

Figure 5. *a*, Epicentres of 281 aftershocks which have occurred during 2004. *b*, Hypocentral depth plot of earthquakes in N–S direction.

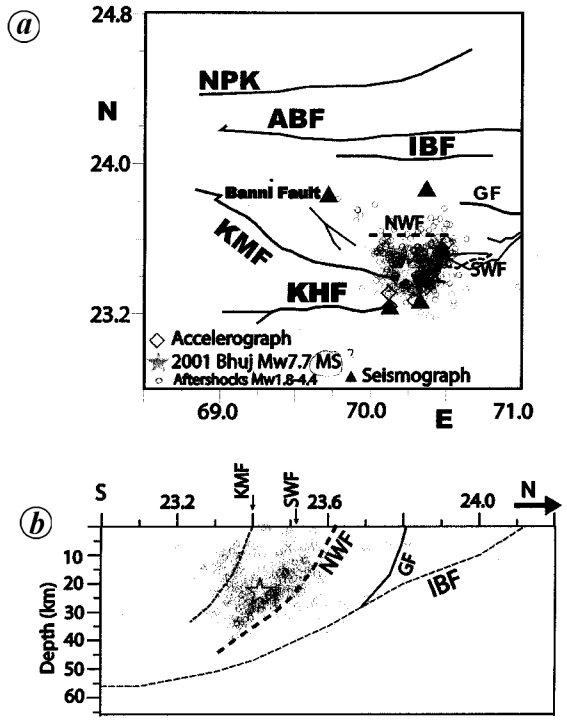

Figure 6. *a*, Epicenters of 585 aftershocks which have occurred during 2005. *b*, Hypocentral depth plot of earthquakes in N–S direction.

The aftershocks include seven *M*4, 39 *M*3 and 26 *M*2 events (Figure 8 *a*). These events are shallow in nature, where focal depths vary from 0 to 15 km. Thus the source for these events is drastically different in comparison to the aftershocks of the 2001 Bhuj earthquake. The hypocentres define an almost vertical fault dipping toward the south coinciding with the spatial location of the earlier mapped E–W trending GF (Figure 8 *b*)[15].

We used a local earthquake moment tensor inversion scheme[22] to compute the source moment-tensor as well as the double-couple components by inverting direct *P*- and *S*-wave amplitudes and polarities for 3, 17 and 19 February as well as 7 March 2006 events. Inputs required for the moment tensor inversions of local earthquakes are amplitudes (in μm) and polarities of *P* (from vertical), *SH*

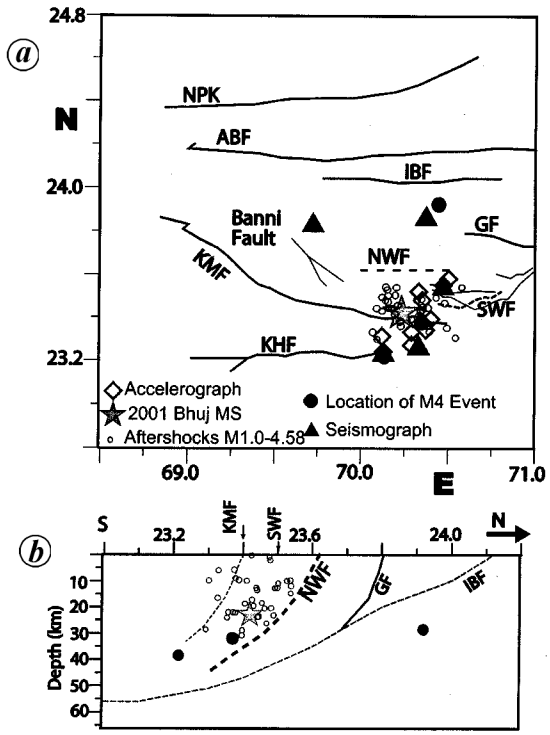

Figure 7. *a*, Epicentres of 42 aftershocks which have occurred during 1 January–6 March 2006. *b*, Hypocentral depth plot of earthquakes in N–S direction.

Table 2. Focal mechanism solutions

Event	Depth (km)	Fault plane	Strike	Dip	Rake
03.02.06	28.7	NP1	288.81	17.95	163.04
		NP2	34.99	84.84	72.78
17.02.06	34	NP1	173.8	32.7	172.7
		NP2	269.9	86.1	57.5
19.02.06	24	NP1	354.7	47.0	32.4
		NP2	241.3	66.9	132.2
07.03.06	2.2	NP1	33.98	88.52	178.67
		NP2	124.02	88.67	1.49

(from transverse) and *SV* (from radial). These inputs were inverted in a linear least squares sense for the five independent components of a traceless moment tensor. This moment tensor was then decomposed into the largest possible double-couple moment tensor and a remaining compensated linear vector dipole tensor[23]. Finally, the resulting double-couple moment tensor was interpreted for the seismic moment, strike, dip and rake. The inversion scheme was applied iteratively until the rms error between the observed and the calculated amplitudes was minimized.

For each of the 3, 17 and 19 February as well as the 7 March 2006 events, a total of 20 datapoints (12 *P*s and 8 *SH*s) were used for the inversion, which led to rms of the order of 0.26 μm. The focal mechanism solutions for the above-mentioned four events are listed in Table 2 and are shown in Figure 8*b*. The 7 March event, which occurred along the GF, suggests a pure strike-slip fault, whereas the focal mechanisms for the 17 and 19 February events, which occurred along the NWF, suggest a reverse fault with a minor strike-slip component along a preferred south-dipping fault. The 3 February 2006 *Mw* 4.58 event, which occurred at 28.7 km depth along the IBF, suggests a reverse motion with a minor strike-slip component along a preferred south-dipping fault. The focal mechanism solution for the 2001 *Mw* 7.7 mainshock has been shown in Figure 1, to give some idea about the existing present-day tectonics.

Estimation of earthquake source parameters, *b*- and *p*-values

The source parameters of the earthquakes have been estimated using a spectral technique where spectrum of *SH*-wave from transverse component is analysed to estimate seismic moment (*Mo*), source radius (*r*), stress drop ($\Delta\sigma$) and static slip[24–27]. A window of 5.12 s from the transverse component of the seismogram was used. In order to minimize the spectral energy leakages, a cosine taper of 10% was applied on both sides of the window. We used Fast Fourier Transform to compute the displacement spectra and removed the instrumental effect. Then we visually fitted (Figure 9) the spectra to the logarithm of the functional form of Brune[24]. The *SH* spectra estimated at different SMA stations for 7 March 2006 *Mw* 5.6 event suggest marked variation in frequency, indicating the influence of site amplifications (Figure 9).

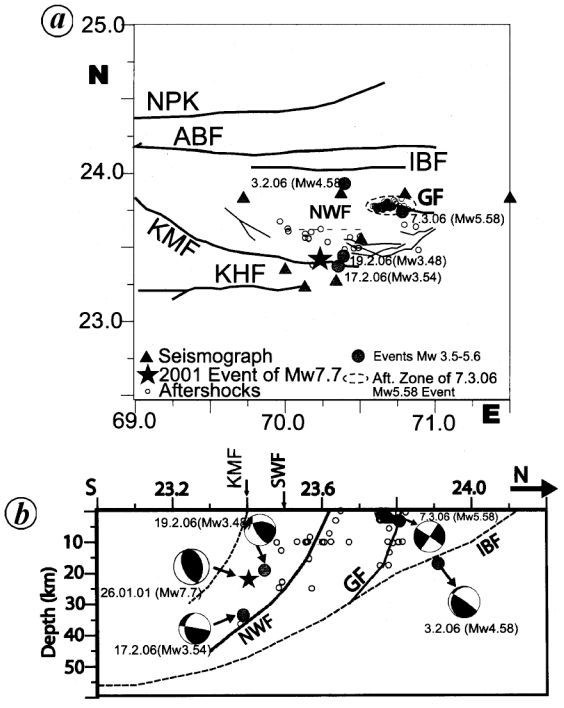

Figure 8. *a*, Epicentres of 72 aftershocks (shown by dotted ellipse) of the 7 March 2006 *Mw* 5.6 event (shown by solid circle), which have occurred during 7–11 March 2006. Solid star shows the epicentre for the 2001 Bhuj main shock. The inferred causative fault is shown by dotted line and marked as NWF. *b*, Hypocentral depth plot of earthquakes in N–S direction. Focal mechanism solutions of 3, 17 and 19 February as well as 7 March 2006 events obtained from local earthquake moment tensor inversion scheme of Ebel[22] are shown. Focal mechanism solution of the 2001 Bhuj main shock is also shown.

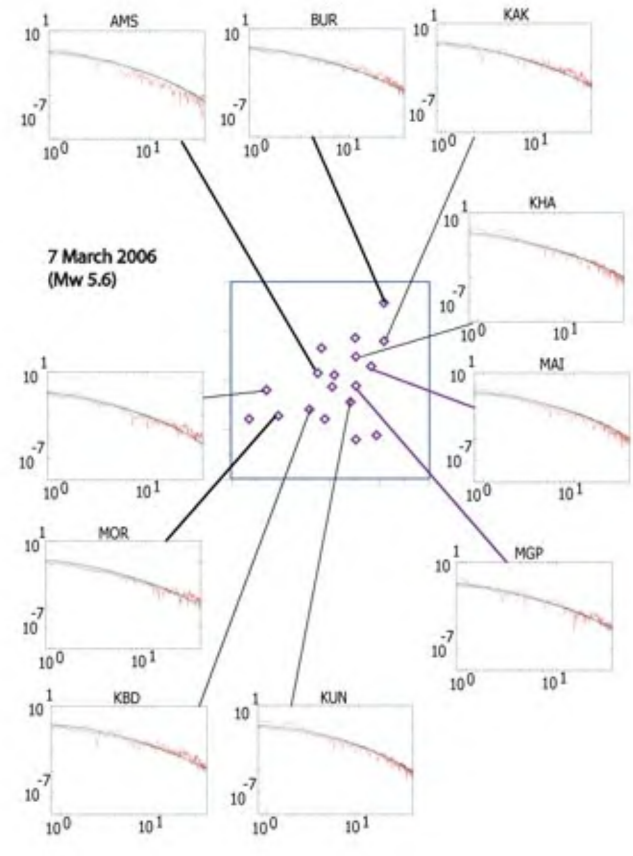

Figure 9. *SH* wave spectra for 7 March 2006 event estimated at ten SMA stations, namely AMS (Amarsar), BUR (Burudia), KAK (Kakarvada), KHA (Kharoi), KUN (Kunjisar), MAI (Mai), BANI (Baniari), MGP (Meghpar), KBD (Kumbardi) and MOR (Morgar).

After obtaining the long-period spectral level (m-s) and corner frequency (Hz) from the observed displacement spectrum of the *SH*-wave at a distance r (in m) and depth h (in m), we estimated the static seismic moment (Mo) using the circular source model of Brune[24]. For estimating the Mo in N-m (1 N-m = 10^7 dyne-cm), we used a *S*-wave velocity (v_s) of 3.6×10^3 m/s, a mean radiation pattern factor ($R_{\theta\phi}$) of 0.55, a density (ρ) value of 2700 kg/m^3, a P factor of $(1/\sqrt{2})$ accounting for the partitioning of energy in the two horizontal components and a free surface amplification factor (F) of 2. A (r, h) accounts for geometrical spreading and κ accounts for the near-surface high-frequency attenuation[28]. $Q(f)$ (= $Q_0 f^n$) takes care of the attenuation related to travel path of seismic waves in terms of frequency-dependent quality factor. For this study, a frequency-dependent relationship ($Q = 102 f^{0.98}$) was obtained from the coda-Qc study using Bhuj aftershocks[29]. For estimating Mo, we also assumed that the geometrical spreading term equals to $(1/R)$, in predicting ground motion for dominance of body waves for $R \leq 100 \times 10^3$ m (~ roughly twice the crustal thickness), where R denotes the epicentral distance of the station (in m). Figures 5 and 6 show a good fit between observed and predicted spectra, indicating the robustness of our estimates for source parameters. We estimated other source parameters like stress drop (in MPa), source radius (in m) and moment magnitude (Mw) for aftershocks using analytical formulas given by Madriaga[25], Keilis Borok[26], and Hanks and Kanamori[27] for a w^2-source model and far-field observation, where the source spectrum of an earthquake is completely specified by its seismic moment and stress drop.

In general, the error in source parameter estimates is analysed by estimating the standard deviation and mean of Mo, r and $\Delta\sigma$. First, the mean of Mo and r were estimated using the procedure described by the Archuleta *et al.*[30]. We further estimated the multiplicative error factor, E_{mo} as defined by Archuleta *et al.*[30]. Following a similar procedure as discussed above for Mo, we estimated average corner frequency and its standard deviation. Then, the source radius was computed using Brune's relation for circular source[24] (equation 5) and the estimated corner frequency at each station. Then the technique of Archuleta *et al.*[30] was used to estimate the S.D. of r.

Finally, adopting the procedure of Fletcher *et al.*[31], the standard deviation of $\Delta\sigma$ was estimated using the formula:

$$\sigma_{std} = \Delta\sigma \sqrt{((\sigma_m/Mo)**2 - 9(\sigma_r/r)**2)}. \quad (1)$$

Following the above-discussed procedure, the standard deviations of (Mo, fc, r and $\Delta\sigma$) and error factor E_{mo} were estimated for the aftershocks recorded at 15 SMA and five broadband seismograph stations. The estimated σ_{fc} (σ_r) for 17 and 19 February 2006 was 0.3 Hz (0.03 m) and 0.4 Hz (0.04 m) respectively. Whereas the error factor E_{mo} of seismic moment for 17 and 19 February events was 1.735 and 1.746 respectively. The estimated σ_{std} for 17 and 19 February events was 0.3 and 0.4 MPa respectively, (1 MPa = 10 bars). The estimated σ_{fc}, σ_r and σ_{std} for the 7 March 2006 event which occurred along the GF were 0.25 Hz, 0.035 m and 0.45 MPa respectively. While the estimated σ_{fc}, σ_r and σ_{std} for the 3 February 2006 event which occurred along the IBF were 0.4 Hz, 0.05 m and 0.5 MPa respectively.

The *SH* spectra for 3, 17 and 19 February as well as the 7 March events were estimated at different stations; as an example we show *SH* spectra for the 7 March 2006 event estimated at 10 SMA sites (Figure 9). Spectra show variable nature for different stations, suggesting significant effect of site response at different sites. The mean of the source parameters estimated at different stations are listed in Table 3.

The least squares and maximum-likelihood methods were used to determine the b-value[10,32]. The maximum-likelihood method gives a better estimate of the b-value than the least squares method, and the estimate[10] is stable for the number of events exceeding 50. Using this method, the b-value is defined as

$$b = \log_{10}e/(M_{av} - M_c), \quad (2)$$

where M_{av} is the average magnitude for each subset and M_c is the lower magnitude limit used in the analysis and $\log_{10}e = 0.4343$. The error (δb) of b-value in 95% confidence limit is determined using the relation suggested by Aki[27]:

$$\delta b = 1.96\, b/\sqrt{n}. \quad (3)$$

For $M \geq 3$ catalogue of Bhuj aftershocks, M_c was estimated using the Gutenberg–Richter power law distribution of magnitude and found to be 3.0 with 90% confidence. The b-value for the complete 2001 Bhuj aftershock se-

Table 3. Estimated mean source parameters for 3, 17 and 19 February as well as 7 March 2006 events

Events	Mean fc (Hz)	Mean seismic moment (dyne-cm)	Mean source radius (m)	Mean stress drop (MPa)	Mean Mw	Number of stations used
03.2.06	6.2 ± 0.84	1.12E + 23	353 ± 57	70.4	4.58 ± 0.23	12
17.2.06	4.9 ± 0.39	2.64E + 21	463 ± 35	1.26	3.54 ± 0.16	20
19.2.06	5.8 ± 0.43	2.00E + 21	394 ± 32	1.49	3.48 ± 0.14	20
07.3.06	1.3 ± 0.15	2.84E + 24	1515 ± 317	26.7	5.60 ± 0.11	18

quence (2001–05) was 0.77 ± 0.02 (Figure 10 *a*). However, for the $M \geq 2.5$ catalogue of the 7 March aftershock sequence, M_c was estimated to be 3.4 with 90% confidence. The cumulative energy release for this event suggests a release of 5.2×10^{24} ergs within 90 h after the occurrence of the 7 March 2006 event (Figure 11 *a*). It also shows maximum release during 60–65 h after the occurrence of the main shock. The *b*-value for the 7 March 2006 aftershock sequence was 0.81 ± 0.1 (Figure 11 *b*). Thus, the *b*-value for the 2001 Bhuj aftershock zone is smaller than that for the aftershock zone of the 7 March 2006 event, suggesting a relatively greater probability of large earthquakes in the aftershock zone of the 2001 Bhuj earthquake in comparison to the aftershock zone of 7 March 2006 of *Mw* 5.6. Thus, the estimated *b*-value of 0.77 or 0.81 is quite less than the average *b*-value of 1.0 for the Indian SCR earthquakes (Table 4), suggesting a relatively greater probability of large earthquakes in the Kachchh region in comparison to other SCRs of India.

The occurrence rate of aftershock sequences is empirically well described by the modified Omori law[10]:

$$n(t) = K/(t + c)^p, \quad (4)$$

where $n(t)$ is the frequency of earthquakes per unit time, at time t after the main shock, and K, c, p are constants. This relation provides a good fit to decay rate (Figures 10 *b* and 11 *c*). The *p*-value for the whole 2001 Bhuj aftershock sequence (2001–05) was estimated to be 0.99, whereas the *p*-value for the aftershock sequence of 7 March event was 0.88 (Figures 10 *b* and 11 *c*). It is important to note that the *p*-value for the aftershock sequence of 1993 *Mw* 6.3 Latur earthquake[33] was 0.9. Hence, it can be inferred that the estimated *p*-value of 0.88 or 0.99 for the Indian intraplate earthquakes is less than the global median[11] of 1.1. The estimated low *p*-values for the aftershock sequences of 2001 NWF and 2006 GF events support the slow decay of aftershock activity.

The 26 January 2001 *Mw* 7.7 Bhuj earthquake took place along the south-dipping NWF in a reverse sense of motion at 23 km depth. The aftershock activity has been continuing even after 5 years of occurrence of the main shock, suggesting a heterogeneous, highly deformed fault zone. Existing seismological data suggest that majority of Kachchh intraplate earthquakes can be attributed to the sudden

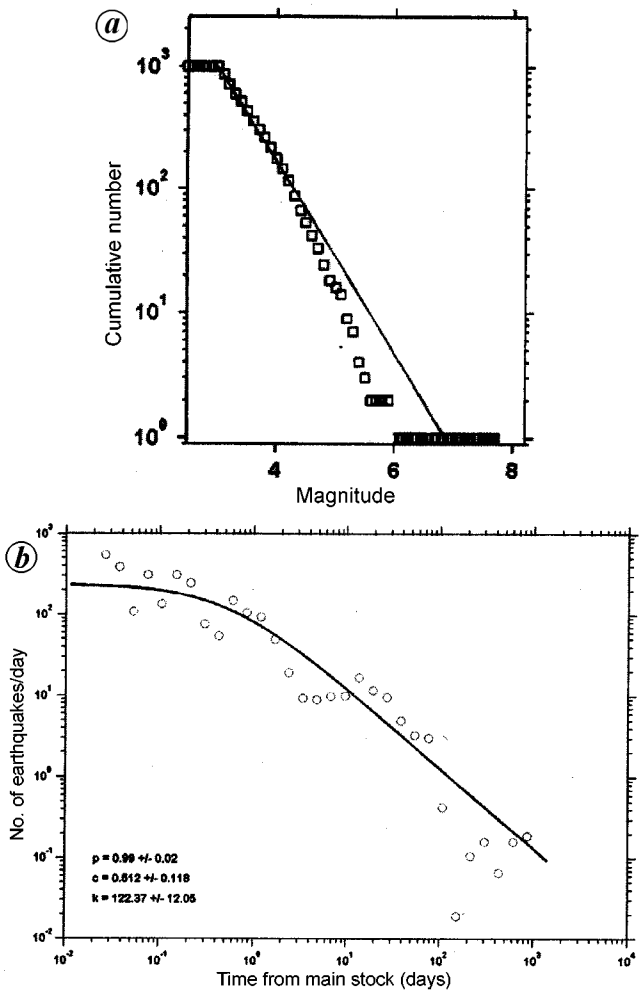

Figure 10. *b*- and *p*-values for the $M \geq 3$ Bhuj aftershocks (26 January 2001 to 31 December 2005). ***a***, Frequency–magnitude plot to show *b*-value estimated from maximum likelihood technique. ***b***, Aftershock decay plot showing *p*-value using modified Omori law.

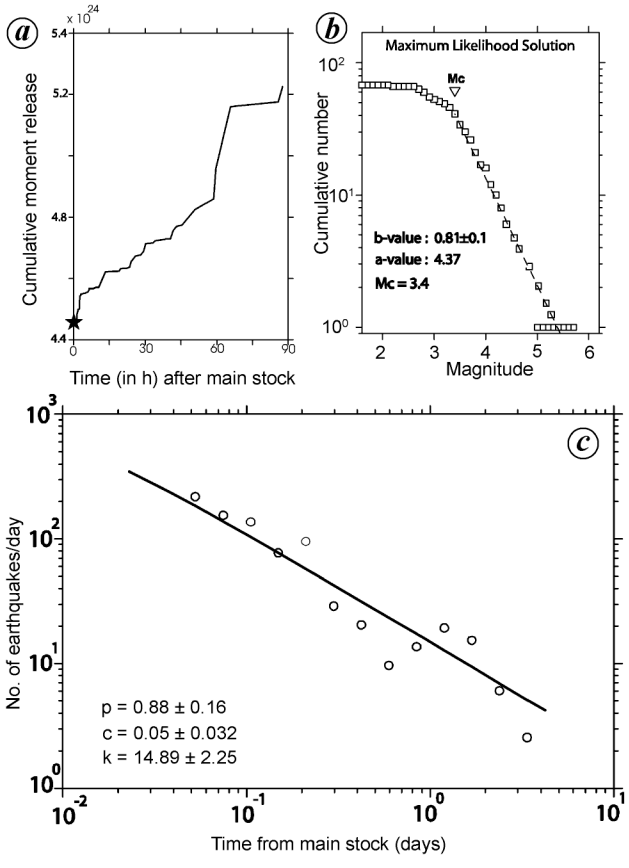

Figure 11. *b*- and *p*-values for the 7 March 2006 aftershock sequence (7–11 March 2006). ***a***, Cumulative energy plot; ***b***, frequency–magnitude plot to show *b*-value estimated from maximum likelihood technique; ***c***, aftershock decay plot showing *p*-value using modified Omori law.

Table 4. Seismic parameters of aftershock sequences for some intraplate earthquakes in India

Earthquake	MS	Aft. max	Aft. max/MS	MS-Aft. max	*b*	Mogi's type
Latur,1993	6.3	5.2	0.84	1.1	0.47	Type-I
Jabalpur, 1997	5.8	4.4	0.76	1.4	0.49	Type-I
Broach,1970	5.4	4.2	0.77	1.2	0.4	Type-I
Idukki, 1985	4.5	4.2	0.93	0.3	0.59	Type-I
Bhuj, 2001	7.8	5.8	0.74	2.0	0.77	Type-II
Koyna, 1967–2000	6.3	5.6	0.9	0.7	1.0	Type-II
Bhatsa, 1984	4.9	4.0	0.8	0.9	0.9	Type-III

MS, Magnitude of mainshock; Aft. max, Magnitude of largest aftershock.

movement along the E–W trending pre-existing reverse/thrust faults in response to the prevailing N–S compression due to the northward movement of the Indian plate[14,15]. Nevertheless, the region is characterized by several uplifts associated with gravity and magnetic highs, which are generally being attributed to crustal intrusive bodies[34]. The results from local earthquake tomography and inversion of teleseismic body waves suggest mafic intrusive high-velocity crustal bodies beneath the aftershock zone[35,36], which could act as a stress concentrator providing large strain energy in the lower crust[3]. Hence, it is apparent from the above discussions that seismicity at the Kachchh rift basin is due to a combination of regional tectonics and local spatial variation of stresses associated with the tectonic structures, which probably originated due to earlier rifting (~140 Ma), followed by Deccan volcanism (65 Ma).

The precisely located aftershocks suggest that the continued aftershock activity has triggered the neighbouring faults in the north like the GF and the IBF. With the passage of time (from 2001 to 2005), the activity became relatively more prominent on the neighbouring KMF in the south. The GF began to experience strong events since August 2003, where a large event of *M*4.5 occurred on 5 August 2003. In 2004, there were infrequent occurrences of events of magnitude ranging from 2.0 to 4.4. In 2005, the activity along GF was subdued, with the occurrences of one *M*3, three *M*2 and four *M*1 events. During January–February 2006, there was no activity along the GF. The activity started in the first week of March, which was followed by a strong earthquake of *M*5.6 on 7 March 2006. Until 11 March 2006, there were 72 aftershocks, including seven *M*4, 39 *M*3 and 26 *M*2 events. This aftershock activity was confined to the upper crust (0–15 km). Seismic activity on the IBF at 30–40 km depth started in 2001, but became intense in 2002–03 over the whole IBF at 10–55 km depth. In 2004, the IBF began to experience the strong earthquakes at 20–50 km depth. The IBF remained active at 15–40 km depth in 2005. During the first two and half months in 2006, the IBF had already experienced two strong events of *Mw* 4.2 and 4.58. Surprisingly, these two strong earthquakes were not associated with any smaller events along the IBF. This led us to an obvious question: 'Is this condition indicative of larger earthquakes along the IBF in future?'.

The moment tensor solutions for 3 February (on the IBF), 17 February (on the NWF) and 19 February (on the NWF) and 7 March 2006 (on the GF) events have been estimated using *P*, *SH* and *SV* amplitudes and polarities. The south-dipping NWF and IBF are found to be reverse in nature, whereas the GF shows a strike-slip behaviour. The aftershock locations on the GF also suggest an almost vertical seismic trend, with a vertical strike-slip fault.

The source parameters for these four strong earthquakes have been studied using the spectral analysis of *SH* wave from the transverse component. The estimated seismic moment, source radius and stress drop for these four events of magnitude 3.48 to 5.6 range from 2.0×10^{21} to 2.84×10^{24} dyne-cm, 353 to 1515 m and 12.6 to 704 bar respectively (Table 3). However, the maximum stress drop value is estimated to be 704 bar for the 3 February event of *Mw* 4.58, which occurred along the IBF at 28.7 km depth. It will be important to note that the epicentre of the 3 February event lies beneath the BANNI sediment, which perhaps resulted in errors in the estimation of corner frequency. Thus, the estimated source parameters for the 3 February event have more errors. The *Mw* 5.6 event of 7 March 2006, which occurred on the GF at 2.2 km depth, gives a stress drop of 267 bar. The 17 and 19 February events, which occurred on the NWF, show a stress drop of 12.6 and 14.2 bar respectively. The kappa value (which provides an estimate of near-surface attenuation) varies from 0.025 to 0.03 for the region.

The estimated *b*-values of 0.77 for aftershocks of 26 January 2001 Bhuj earthquake of *Mw* 7.7 and 0.81 for aftershocks of 7 March 2006 GEDI event of *Mw* 5.6 are much less than the average *b*-value of 1.0 for the Indian SCR earthquakes (Table 2), suggesting a relatively higher probability of large earthquakes in the Kachchh region in comparison to other SCRs of India. According to Mogi's classification[37], the range of *b*-value in Mogi type-I sequences is 0.4–0.6. For Mogi type-II sequences, *b*-value lies in the range 0.6–1.2, whereas in Mogi type-III sequences, *b*-value lies in the range 0.85–1.00. Thus, *b*-value (ratio of frequency of small to large magnitude earthquakes) distribution indicates that Mogi type-I sequences (mainshock followed by aftershock activity) are in highly stressed regions with concentrated stresses and homogeneous rocks. Mogi type-III sequences show swarm activity

is uniformly stressed regions and heterogeneous rocks. Mogi type-II sequences are in the regions of intermediate level stresses and heterogeneity. Mogi type-III sequences show lowest release of energy (10–20%) in the main shocks, whereas Mogi type-I sequences show maximum energy (60–90%) liberated in main shocks compared to the aftershocks. Mogi type-II sequences lie between them with 30–60% strain energy released during the main shock. Thus, based on the above discussion the aftershock sequences of the 2001 Bhuj earthquake and 2006 GEDI event could be categorized as the Mogi's type-II sequences, indicating a region of intermediate-level stresses and heterogeneous rocks.

It is well known that the p-value of the Omori law[10] is the exponent of the decay of frequency of aftershocks with time. The Omori law of aftershock decay states that the frequency of aftershocks decays as the reciprocal of time following the mainshock[38]. Elastic stress changes, such as those exerted on a fault by a large earthquake, act instantaneously and by themselves cannot explain the time dependence of aftershocks; however, there are several possible physical mechanisms that can give rise to the observed time dependence such as pore fluid diffusion[39], rate and state variable friction[40] and loading rate due to creep[41]. The estimated p-value for the complete aftershock sequence (26 January 2001–31 December 2005) was 0.99 (Figure 10 *b*). Whereas the p-value for the aftershock sequence of 2006 GEDI event was 0.88. Thus, both the aftershock sequences of 2001 Bhuj and 2006 GEDI events suggest a relatively slow decay. However, the continued occurrence of aftershocks of 2001 Bhuj earthquake makes this sequence unique and complex, and different from the 2006 GEDI aftershock sequence. It will be important to note that a recent theoretical modelling of aftershock activity by Zoller *et al.*[42], suggests that any complex aftershock sequence can be explained in terms of a model consisting of brittle fault segments separated by creeping zones. They also suggested that the ratio of creep coefficients in the brittle and creeping sections determines the duration of the post-seismic transients and the exponent 'p' of the modified Omori law. Therefore, it is inferred based on the above discussion that a decrease in p-value and an increase in aftershock zone, both spatially as well as in depth over the passage of time, suggest that the decay of aftershocks of the 2001 Bhuj earthquake could be controlled by visco-elastic creep in the lower crust[42].

Major E–W trending faults characterize the seismotectonics of the Kachchh region. Available earthquake data reveal that dominant deformation mode for the region is south-dipping thrust faulting. In accordance with dominant E–W trends, aftershock locations during January 2001–March 2006 suggest on an average an E–W trending, south-dipping aftershock zone extending up to 40 km depth. Variation in focal depth distributions of aftershocks during the above-mentioned period suggests that main aftershock zone has become deeper over the passage of time, with increase in the size of the zone. Based on the study of temporal distribution (2001–06) of earthquakes along the NWF, IBF and GF, it is inferred that the 3 February 2006 event along the IBF and 7 March 2006 event along the GF were triggered by the five years continued aftershock activity of the 2001 Bhuj event of Mw 7.7. The 7 March 2006 event of Mw 5.6 that occurred at 2.2 km along the almost vertical GF suggests a strike-slip sense of motion and a large stress drop of 26.7 MPa. The 3 February 2006 event of Mw 4.58, which occurred at 28.7 km depth along the south-dipping IBF, suggests a reverse sense of motion and an anomalously large stress drop of 70.6 MPa. The 17 and 19 February 2006 events of Mw ~3.7, which occurred on the south-dipping NWF, suggest a reverse sense of motion and a smaller stress drop of the order of 1.5 MPa. Thus the region is characterized by large stress drop values, which could be attributed to the existence of crustal rigid, brittle mafic intrusive bodies.

The estimated b-value of 0.77 and 0.81 for the 2001 Bhuj and 2006 GEDI sequences is less than the average b-value of 1.0 for the Indian SCR earthquakes (Table 2), suggesting probability of large earthquakes in the Kachchh region in comparison to other SCRs of India. Thus, these two aftershock sequences could be categorized as the Mogi's type-II sequences, indicating a region of intermediate-level stresses and heterogeneous rocks. The p-value for the 2001–05 and the 2006 sequences was 0.99 and 0.88 respectively, which is less than the global median of 1.1 that supports the slower decay of aftershocks for the studied sequences. It is inferred that the decrease in p-value and increase in aftershock zone, both spatially as well as depth over the passage of time, suggests that the decay of aftershocks perhaps could be controlled by visco-elastic creep in the lower crust.

1. Johnston, A. C., Seismotectonic interpretations and conclusions from the stable continental regions. In *The Earthquakes of Stable Continental Regions: Assessment of Large Earthquake Potential*, Electric Power and Research Institute, Palo Alto, 1994.
2. Kane, M. F., Correlation of major eastern earthquake centers with mafic/ultra-mafic basement masses. USGS Prof. Pap., 1977, p. 1028.
3. Campbell, D. L., Investigation of the stress concentration mechanism for intraplate earthquakes. *Geophys. Res. Lett.*, 1978, **5**, 477–479.
4. Schweig III, E., Gomberg, J., Petersen, M., Ellis, M., Bodin, P., Mayrose, L. and Rastogi, B. K., The *M* 7.7 Bhuj earthquake: Global lessons for earthquake hazard in intra-plate regions. *J. Geol. Soc. India*, 2003, **61**, 277–282.
5. Rajendran, C. P. and Rajendran, K., Character of deformation and past seismicity associated with the 1819 Kachchh earthquake, northwestern India. *Bull. Seismol. Soc. Am.*, 2001, **91**, 407–426.
6. Mogi, K., Magnitude-frequency-relation for elastic shocks accompanying fractures of various materials and some related problems in earthquakes. *Bull. Earthquake Res. Inst., Univ. Tokyo*, 1962, **40**, 831–853.
7. Scholtz, C. H., The frequency–magnitude relation of microfracturing in rock and its relation to earthquakes. *Bull. Seismol. Soc. Am.*, 1968, **58**, 399–415.

8. Warren, N. W. and Latham, G. V., An experimental study of thermally induced microfracturing and its relation to volcanic seismicity. *J. Geophys. Res.*, 1970, **75**, 4455–4464.
9. Wiemer, S. and Wyss, M., Mapping spatial variability of the frequency–magnitude distribution of earthquakes. *Adv. Geophys.*, 2002, **45**, 259–302.
10. Utsu, T., A statistical study on the occurrence of aftershocks. *Geophys. Mag.*, 1961, **30**, 521–605.
11. Utsu, T., Ogata, Y. and Matsu'ura, R. S., The centenary of the Omori formula for a decay law of aftershock activity. *J. Phys. Earth*, 1995, **43**, 1–33.
12. Gupta, H. K. *et al.*, Bhuj earthquake of 26 January 2001. *J. Geol. Soc. India*, 2001, **57**, 275–278.
13. Biswas, S. K. and Deshpande, S. V., Geological and tectonic maps of Kachchh. *Bull. Oil Nat. Gas Comm.*, 1970, **7**, 115–116.
14. Chung, W. Y. and Gao, H., Source parameters of the Anjar earthquake of 21 July 1956, India and its seismotectonic implications for the Kutch rift basin. *Tectonophysics*, 1995, **242**, 281–292.
15. Biswas, S. K., Regional framework, structure and evolution of the western marginal basins of India. *Tectonophysics*, 1987, **135**, 302–327.
16. Reddy, P. R., Sarkar, D., Sain, K. and Mooney, W. D., A report on a collaborative scientific study at USGS, Menlo Park, USA (30 October–23 December 2001), 2001, p. 19.
17. Mandal, P., Receiver function analysis of teleseismic *P*-waves: Implication toward sedimentary basin and Moho depth variation beneath Kachchh and Saurashtra regions, Gujarat (India). *Phys. Earth Planet. Int.*, 2006, **155**, 286–299.
18. Mandal, P. and Pujol, J., Seismic imaging of the aftershock zone of the 2001 *Mw* 7.7 Bhuj earthquake, India. *Geophys. Res. Lett.*, 2006, **33**, 1–4.
19. Mandal, P., Horton, S. and Pujol, J., Relocation, V_p and V_p/V_s tomography, focal mechanisms and other related studies using aftershock data of the *Mw* 7.7 Bhuj earthquake of 26 January 2001. *J. Indian Geophys. Union*, 2006, **10**, 31–44.
20. Kayal, J. R. *et al.*, The 2001 Bhuj earthquake: Tomographic evidence for fluids at the hypocenter and its implications for rupture nucleation. *Geophys. Res. Lett.*, 2002, **29**, 5-1–5-4.
21. Bodin, P. and Horton, S., Source parameters and tectonic implications of aftershocks of the *Mw* 7.6 Bhuj earthquake of 26 January 2001. *Bull. Seismol. Soc. Am.*, 2004, **94**, 818–827.
22. Ebel, J. E., The effect of crustal scattering on observed high frequency earthquake seismograms. *Geophys. J.*, 1989, **95**, 1024–1035.
23. Langston, C. A., Source transmission of seismic waveforms: The Koyna, India earthquakes of 13 September 1967. *Bull. Seismol. Soc. Am.*, 1981, **71**, 1–24.
24. Brune, J., Tectonic stress and the spectra of seismic shear waves from earthquakes. *J. Geophys. Res.*, 1970, **75**, 4997–5009.
25. Madriaga, R., Dynamics of an expanding circular fault. *BSSA*, 1976, **66**, 639–666.
26. Keilis Borok, V. I., On the estimation of the displacement in an earthquake source and of source dimensions. *Ann. Geofis.*, 1959, **19**, 205–214.
27. Hanks, T. C. and Kanamori, H., A moment magnitude scale. *J. Geophys. Res. B*, 1979, **84**, 2348–2350.
28. Singh, S. K., Apsel, R. J., Fried, J. and Brune, J. N., Spectral attenuation of SH-waves along the Imperial fault. *Bull. Seismol. Soc. Am.*, 1982, **72**, 2003–2016.
29. Mandal, P., Jainendra, Joshi, S., Kumar, S., Bhunia, R. and Rastogi, B. K., Low coda-*Qc* in the epicentral region of the 2001 Bhuj earthquake of *Mw* 7.7, *PAGEOPH*, 2004, **161**, 1635–1654.
30. Archuleta, R. J., Cranswick, E., Muellar, C. and Spudich, P., Source parameters of the 1980 Mammoth lakes, California, earthquake sequence. *J. Geophys. Res.*, 1982, **87**, 4595–4607.
31. Fletcher, J. B., Boatwright, J., Harr, Linda, Hanks, T. and Macgarr, A., Source parameters for aftershocks of the Oroville, California, earthquake. *Bull. Seismol. Soc. Am.*, 1984, **74**, 1101–1123.
32. Aki, K., Maximum likelihood estimate of b in the formula $\log N = a - bM$ and its confidence limits. *Bull. Earthquake Res. Inst. Univ. Tokyo*, 1965, **43**, 237–239.
33. Baumbach, M. *et al.*, Study of the foreshocks and aftershocks of the intraplate Latur earthquake of 30 September 1993, India. *Mem. Geol. Soc. India*, 1994, **35**, 33–63.
34. Chandrasekhar, D. V. and Mishra, D. C., Some geodynamic aspects of Kutch basin and seismicity: An insight from gravity studies. *Curr. Sci.*, 2002, **83**, 492–498.
35. Mandal, P., Rastogi, B. K., Satyanarayana, H. V. S. and Kousalya, M., Results from local earthquake velocity tomography: Implications toward the source process involved in generating the 2001 Bhuj earthquake in the lower crust beneath Kachchh (India). *Bull. Seismol. Soc. Am.*, 2004, **94**, 633–649.
36. Antolik, M. and Dreger, D. S., Rupture process of the 26 January 2001 *Mw* 7.6 Bhuj, India, earthquake from teleseismic broadband data. *Bull. Seismol. Soc. Am.*, 2003, **93**, 1235–1248.
37. Mogi, K., Magnitude–frequency relation for elastic shocks accompanying fractures of various materials and some related problems in earthquakes. *Bull. Earthquake Res. Inst., Univ. Tokyo*, 1962, **40**, 831–853.
38. Scholz, C. H., *The Mechanics of Earthquakes and Faulting*, Cambridge University Press, New York, 1990, p. 439.
39. Nur, A. and Booker, J. R., Aftershocks caused by pore fluid flow? *Science*, 1972, **175**, 885–887.
40. Dieterich, J. H., A constitutive law for earthquake production and its application to earthquake clustering. *J. Geophys. Res.*, 1994, **99**, 2601–2618.
41. Schaff, D. P., Beroza, G. C. and Shaw, B. E., Postseismic response of repeating aftershocks. *Geophys. Res. Lett.*, 1998, **25**, 4549–4552.
42. Zoller, G., Hainzl, S., Holschneider, M. and Ben-Zion, Y., Aftershocks resulting from creeping sections in a heterogeneous fault. *Geophys. Res. Lett.*, 2005, **32**, L03308.

ACKNOWLEDGEMENTS. We thank to Dr V. P. Dimri, Director, NGRI, Hyderabad for encouragement and permission to publish this work. This study was supported by the Department of Science and Technology, New Delhi.

Received 1 April 2006; revised accepted 4 December 2006